High-order residual distribution : discontinuity capturing crosswind dissipation and diffusion

N. Villedieu-Ligout[1], M. Ricchiuto[2], and H. Deconinck[1]

[1] von Karman Institute for Fluid Dynamics
nadege.villedieu@vki.ac.be, deconinck@vki.ac.be
[2] INRIA Futurs, project ScAlApplix and MAB, Université de Bordeaux I
Mario.Ricchiuto@inria.fr

1 Generalities and notation

We review a class of compact methods to approximate steady solutions to

$$\frac{\partial u}{\partial t} + \nabla \cdot \mathcal{F}(u) = \nabla \cdot (\nu \nabla u) \quad \forall (x,y) \in \Omega \tag{1}$$

on τ_h, an unstructured triangulation of the domain Ω. We make use of standard Lagrangian P^k elements, that is the solution is approximated by a continuous piecewise k-th order polynomial. In every triangle $T \in \tau_h$ we construct the sub-triangulation composed by k^2 triangles shown on figure 1. We denote by T_s the generic sub-element.

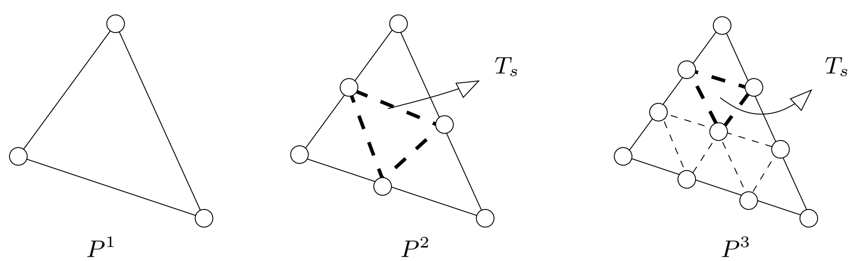

Fig. 1. P^k Lagrangian triangles with P^1 conformal sub-triangulation

On τ_h, the discrete unknown u^h is expressed as the following combination of k-th Lagrangian polynomial basis functions :

$$u^h(x,y) = \sum_{i \in \tau_h} u_i \psi_i(x,y) \tag{2}$$

where $u_i = u(x_i, y_i)$ and ψ_i the i-th basis function. We call φ_i the piecewise linear basis function associated to $i \in T$ defined on the P^1 conformal sub-triangulation (see figure 1). Clearly, in the P^1 case $\varphi_i = \psi_i$.

We consider schemes evolving the nodal values of the solution as :

$$u_i^{n+1} = u_i^n + \delta_i \sum_{T_s, i \in T_s} \Phi_i^{T_s} \tag{3}$$

where δ_i is an iteration parameter. In the hyperbolic case $\nu = 0$, the schemes we consider are a particular case of the fluctuation or residual distribution ($\mathcal{RD}$) schemes of [AR03]. In particular, on every sub-element T_s we have

$$\sum_{j \in T_s} \Phi_j^{T_s} = \Phi^{T_s} = \int_{T_s} \nabla \cdot \mathcal{F}_h(u^h)\, dx\, dy \tag{4}$$

The paper is divided in two parts. In the first one we show the general construction of $k+1$-th order schemes for hyperbolic scalar conservation laws. The extension to (1) is considered in the second part.

2 Quasi non-oscillatory $\mathcal{RD}$ for hyperbolic problems

First consider (1) in the hyperbolic case $\nu = 0$. We review some $\mathcal{RD}$ schemes satisfying all the following conditions:

Accuracy Condition to get $k+1$-th order schemes is that (see [AR03] for details)

$$\Phi_j^{T_s} = \mathcal{O}(h^{k+2}) \tag{5}$$

For the k-th degree polynomial approximation (2) we get $\Phi^{T_s} = \mathcal{O}(h^{k+2})$, hence the accuracy condition is also expressed by $\Phi_j^{T_s} = \mathcal{O}(\Phi^{T_s})$

Upwinding In T_s, let $\mathbf{n}_i$ be the inward normal to the edge facing node i scaled by the length of the edge. Upwind schemes are the ones for which

$$k_i \leq 0 \Rightarrow \Phi_i^{T_s} = 0\,, \quad \text{with } k_i = \frac{1}{2}\frac{\partial \mathcal{F}(u^*)}{\partial u} \cdot \mathbf{n}_i \tag{6}$$

with u^* an arbitrary average of u^h over T_s. Upwinding has a stabilizing effect (see [AR03] for the analysis).

Monotonicity The rigorous definition of monotonicity for $\mathcal{RD}$ schemes resorts to the theory of positive coefficients, see [AR03, RVAD05] for details. In this paper we will define a scheme as being monotone if, in practical computations, it gives a non-oscillatory approximations of discontinuities. In particular, we are interested in schemes for which, across a discontinuity, $\Phi_j^{T_s} \times \Phi_j^{\mathrm{M}} \geq 0$, for some first order monotone splitting Φ_j^{M}.

In the following subsections we review some definitions for the $\Phi_j^{T_s}$s.

2.1 Linear schemes

In this paper we make use of the following two upwind linear schemes

LDA scheme is the upwind scheme defined by

$$\Phi_i^{T_s} = \Phi_i^{\mathrm{LDA}} = \beta_i^{\mathrm{LDA}} \Phi^{T_s}\,, \quad \beta_i^{\mathrm{LDA}} = k_i^+ / \sum_{j \in T_s} k_j^+ \tag{7}$$

Since β_i^{LDA} is uniformly bounded (w.r.t. mesh size h and solution u^h), the LDA scheme respects the accuracy condition (5)

N scheme is the upwind scheme defined by

$$\Phi_i^{T_s} = \Phi_i^{\mathrm{N}} = k_i^+(u_i - u_{in})\,, \quad u_{in} = \big(\sum_{j\in T_s} k_j^+\big)^{-1}\big(\sum_{j\in T_s} k_j^+ u_j - \Phi^{T_s}\big) \quad (8)$$

The N scheme is monotone (in the sense described in section 2) and first order. On can easily show that the N is obtained by adding to the LDA scheme a crosswind (shock capturing) dissipation term [RVAD05] :

$$\Phi_i^{\mathrm{N}} = \Phi_i^{\mathrm{LDA}} + \mathrm{d}_i^{\mathrm{N}}\,, \quad \mathrm{d}_i^{\mathrm{N}} = \big(\sum_{j\in T} k_j^+\big)^{-1} \sum_{j\in T} k_i^+ k_j^+ (u_i - u_j) \qquad (9)$$

2.2 Nonlinear schemes

To combine high order of accuracy and monotonicity, we must define use a nonlinear splitting. There are two ways of doing this :

Blending the LDA and N splittings in a way guaranteeing that the N scheme is recovered only across shocks. For example :

$$\Phi_i^{T_s} = \Phi_i^{\mathrm{B}} = \theta\,\Phi_i^{\mathrm{N}} + (1-\theta)\,\Phi_i^{\mathrm{LDA}}\,, \quad \theta = \frac{|\Phi^{T_s}|}{\sum_{j\in T_s} |\Phi_j^{\mathrm{N}}|} \qquad (10)$$

Due to (9), this is equivalent to add to the LDA scheme a residual shock capturing crosswind dissipation term :

$$\Phi_i^{\mathrm{B}} = \Phi_i^{\mathrm{LDA}} + \theta \mathrm{d}_i^{\mathrm{N}} \qquad (11)$$

Limiting the distribution coefficient of the N scheme (PSI scheme) :

$$\Phi_i^{T_s} = \Phi_i^{\mathrm{PSI}} = \beta_i^{\mathrm{PSI}} \Phi^{T_s}\,, \quad \beta_i^{PSI} = \beta_i^{\mathrm{N},+} / \sum_{j\in T_s} \beta_j^{\mathrm{N},+} \qquad (12)$$

with $\beta_j^{\mathrm{N}} = \Phi_i^{\mathrm{N}}/\Phi_i^{T_s}$. The PSI scheme verifies both the monotonicity requirement ($\Phi_i^{T_s} \times \Phi_i^{\mathrm{N}} \geq 0$), and the accuracy condition (5) (β_i^{PSI} bounded).

2.3 Numerical examples

We show examples involving smooth and non-smooth solutions. First, on the domain $[-1,1]\times[0,1]$, we consider the steady rotation ($\mathcal{F} = \boldsymbol{\lambda} u,\ \boldsymbol{\lambda} = (y\,,-x)$) of the inlet profile $u_0 = \sin(16\pi x)$, defined on the boundary $x \in [-1,0],\ y = 0$. On the left on figure 2, we plot the outlet ($x \in [0,1],\ y = 0$) data computed by the second, third and fourth order PSI schemes. All the computations have been run with *the same number of degrees of freedom*. The improvement in the resolution of the high frequency profile brought by the higher order polynomial representation is evident.

As a second example, the right picture on the same figure shows the grid convergence rates obtained on P^3 elements for the constant advection ($\mathcal{F} = \boldsymbol{\lambda} u,\ \boldsymbol{\lambda} = (0\,,1)$) of $\cos(\pi x)$ on the square $[0,1]^2$. The high order schemes (including the nonlinear ones) yield the expected fourth order of accuracy.

Lastly, figure 3 shows the results obtained on the Burger's equation ($\mathcal{F} = (u^2\,,2u)/2$) on the square $[0,1]^2$ with boundary conditions $u = 1.5 - 2x$ for $y = 0$. On the left we report the contours of the solution obtained with the PSI (P3) schemes, while on the right a cut at $y = 0.75$ of the PSI (P2) and PSI (P3) solutions. Some oscillations are present in very few mesh points after the shock, however, their amplitude is small (below 15% local value of u).

3 Very high order $\mathcal{RD}$ and diffusion terms

We now consider the issue of including the diffusive terms into the discretization. As shown in [Nis05, RVAD05], the main problem is to properly take into account the relative magnitude of transport and diffusion terms, measured by the Peclet number $Pe = h\|\boldsymbol{\lambda}\|/\nu$, with $\boldsymbol{\lambda}$ a local reference wave speed (flux Jacobian). We briefly review the approach of [RVAD05].

The idea is to use $\mathcal{RD}$ only in advection dominated regions, to take advantage of its shock capturing. In diffusion dominated regions, on the other hand, Galerkin and stabilized Galerkin schemes perform very well. The problem is to build Petrov-Galerkin (PG) discretizations consistent with a given $\mathcal{RD}$ scheme, and to combine the two discretizations to obtain uniformly (w.r.t. h and Pe) accurate approximations.

The solution proposed in [RVAD05] is the following. Given a $\mathcal{RD}$ scheme with distribution coefficients $\beta_j^{T_s}$, such that $\Phi_j^{T_s} = \beta_j^{T_s}\Phi_j^{T_s}$, build continuous piecewise polynomial test functions respecting the consistency conditions

$$\frac{1}{|T_s|}\int\limits_{T_s} \omega_j \; dx\, dy = \beta_j^{T_s} \qquad \forall\, j \in T \text{ and } \forall T_s \subset T \tag{13}$$

There are several ways of choosing these functions, however, in a PG context, the most natural way to do it is to define them as perturbations of some basis functions. Here we consider the case in which the ω_js are defined as

$$\omega_j|_{T_s} = \varphi_j + (3\beta_j^{T_s} - 1)S^{T_s} \tag{14}$$

with φ_j piecewise linear basis functions on the conformal P^1 sub triangulation, and S^{T_s} are locally defined *bubble* functions. These perturbations are such that ω_j respects (13) (see [RVAD05] for details). Consider now the compact scheme

$$\begin{aligned}\Phi_i^{T_s} = & \overbrace{\int_{T_s} \varphi_i \lambda \cdot \nabla u^h \; dx\, dy}^{\Phi_i^{\mathrm{C}}} + (\beta_i^{T_s}\Phi^{T_s} - \Phi_i^{\mathrm{C}}) + \\ & \int\limits_{T_s} \nu \nabla u^h \cdot \nabla \varphi_i \; dx\, dy + (3\beta_j^{T_s} - 1)\int\limits_{T_s} \nu \nabla u^h \cdot \nabla S^{T_s} \; dx\, dy \end{aligned} \tag{15}$$

In the last definition, the first line represents the $\mathcal{RD}$ scheme[3], while the second line contains the PG discretization of the diffusive terms. As pointed out in [RVAD05], (15) does not introduce any coupling between the discrete advection operator and diffusion operators. Defining the following discrete Peclet number

$$Pe^h = \frac{|\Phi^{T_s}|}{\sum\limits_{j \in T_s} |\int\limits_{T_s} \nu \nabla u^h \cdot \nabla \varphi_i \; dx\, dy|}$$

[3] the central finite element contribution Φ_i^{C} is added and subtracted for reason which will be soon clear

one can instead use the hybrid discretization :

$$\Phi_i^{T_s} = \Phi_i^{\mathrm{C}} + \int\limits_{T_s} \nu \nabla u^h \cdot \nabla \varphi_i \; dx\, dy +$$

$$\xi(Pe^h)(\beta_i^{T_s}\Phi^{T_s} - \Phi_i^{\mathrm{C}}) + \xi(Pe^h)(3\beta_j^{T_s} - 1) \int\limits_{T_s} \nu \nabla u^h \cdot \nabla S^{T_s} \; dx\, dy \quad (16)$$

with $\xi(\cdot)$ continuous, and such that $\lim_{x\to 0} \xi(x) = 0$ and $\lim_{x\to\infty} \xi(x) = 1$. Scheme (16) reduces to a Galerkin type high order approximation in diffusion dominated regions, while the $\mathcal{RD}$ discretization is recovered in advection dominated solutions. The relative magnitude of these phenomena are measured by a residual based monitor, given by the discrete Peclet number Pe^h.

3.1 Results

The effect of the introduction of the Pe^h scaling is shown on a practical problem. We take $\boldsymbol{\lambda} = (0, 1)$, and the following boundary conditions :

$$u(x,0) = -\cos(2x\pi)\,, \qquad u(x,1) = -\cos(2x\pi)\exp(\frac{1-\sqrt{1+16\pi^2\nu^2}}{2\nu})$$

$$u(0,y) = -\exp(y\frac{1-\sqrt{1+16\pi^2\nu^2}}{2\nu})\,, \quad u(1,y) = -\exp(y\frac{1-\sqrt{1+16\pi^2\nu^2}}{2\nu})$$

We solve the problem on P^2 and P^3 elements. To enhance the effects of the Pe^h scaling, we take $\nu = 10^{-2}$ in the P^2 case, and $\nu = 10^-3$ in the P^3 one.

Figure 4 shows the convergence rates measured for a smooth problem (see [RVAD05] for details on the set up). We use the LDA scheme with formulations (15) and (16) ($\xi = \min(1, Pe^h)$). Without a proper coupling between the advective and diffusive operators there is an evident loss of accuracy. Conversely, scheme (16) clearly yields optimal convergence rates.

References

[RVAD05] Ricchiuto, M., Villedieu, N., Abgrall, R., Deconinck, H.: High-order residual distribution schemes : discontinuity capturing crosswind dissipation and extension to advection-diffusion, VKI LS on Higher Order Discretization Methods for Computational Physics, Von Karman Institute for Fluid Dynamics (2005)

[Abg05] Abgrall, R. : Very high order residual distribution methods,VKI LS on Higher Order Discretization Methods for Computational Physics, Von Karman Institute for Fluid Dynamics (2005)

[Dep05] De Palma, P. : Implicit third-order-accurate residal distribution schemes for unsteady hyperbolic problems, VKI LS on Higher Order Discretization Methods for Computational Physics, Von Karman Institute for Fluid Dynamics (2005)

[Nis05] Nishikawa, H. : Higher order discretization of diffusion terms in residual distribution methods, VKI LS on Higher Order Discretization Methods for Computational Physics, Von Karman Institute for Fluid Dynamics (2005)

[AR03] Abgrall, R., Roe, P.L.: High order fluctuation schemes on triangular meshes. J. Sci. Comput., **19(3)**, 3–36 (2003)

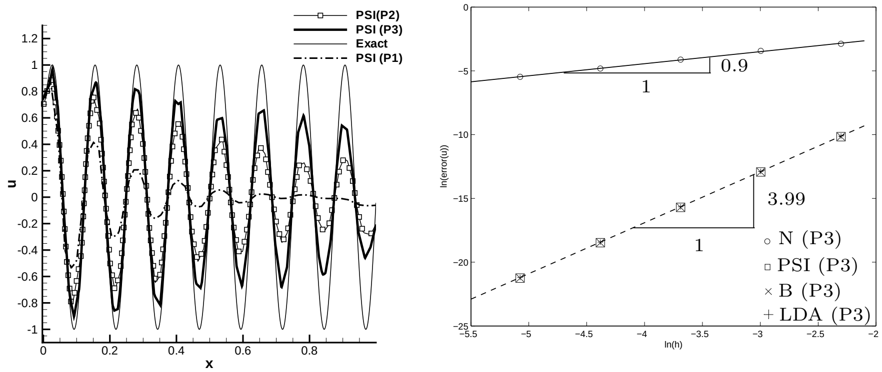

Fig. 2. Rotation of $\sin(16\pi x)$ and grid convergence (constant advection of $\cos(\pi x)$)

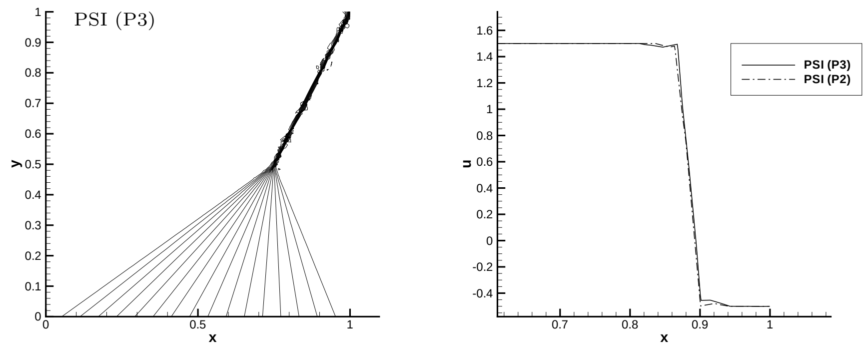

Fig. 3. Burgers equation : PSI (P3) solution contours and cut at $y = 0.75$ of the PSI (P2) ans PSI (P3) solutions

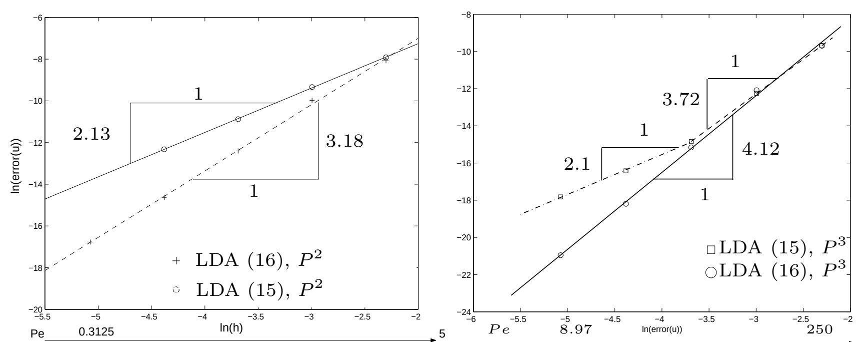

Fig. 4. Advection-diffusion : grid convergence on P^2 (left) and P^3 (right) elements